

Comparisons of Model Predictions of Pion Electrioproduction Amplitudes in the low Q^2 Region

T. Sato^a and T.-S. H. Lee^b

^a *Department of Physics, Osaka University, Toyonaka, Osaka 560-0043, Japan*

^b *Physics Division, Argonne National Laboratory, Argonne, Illinois 60439*

Abstract

Pion electroproduction amplitudes predicted by three theoretical models in the $Q^2 \leq 0.5$ (GeV/c)² region are compared. The objective is to facilitate the analyses of the data from new experiments on investigating the pion cloud effects on the $\gamma N \rightarrow \Delta$ transition form factors.

In recent years, the data of pion electroproduction reactions have been analyzed by using various models for extracting the $\gamma N \rightarrow \Delta$ transition form factors. The large pion cloud effects predicted by the dynamical models[1, 2, 3, 4] have motivated new measurements in the low momentum transfer region $Q^2 \leq 0.5$ (GeV/c)². To facilitate the analyses of these new data, we here compare the predictions from three models : the Sato-Lee(SL) Model[1, 2], the Dubna-Mainz-Taiwan(DMT) model[3, 4], and the Mainz Unitary Isobar Model (MAID)[5]. The details of each of the considered models can be found in their original papers and therefore will not be repeated here. We only point out some noticeable differences between them, which are relevant to the understanding of the pion cloud effects.

I. R_{EM} AND R_{SM} RATIOS OF THE Δ RESONANCE

The deformation of the nucleon and/or Δ is reflected in the non-zero values of the ratios

$$R_{EM} = \frac{[\bar{\Gamma}]_{E2}}{[\bar{\Gamma}]_{M1}} \quad (1)$$

$$R_{SM} = \frac{[\bar{\Gamma}]_{C2}}{[\bar{\Gamma}]_{M1}}, \quad (2)$$

where $[\bar{\Gamma}]_\alpha$ denotes the $\gamma N \rightarrow \Delta$ transition with multipolarity $\alpha = M1$ (magnetic M1), $E2$ (electric E2), and $C2$ (Coulomb C2). As explained, for example, in Ref.[2], these two ratios at the resonance energy $W = m_\Delta = 1232$ MeV can be calculated from the imaginary (Im) parts of the multipole amplitudes of pion electroproduction reactions

$$R_{EM} = \frac{Im[E_{1+}^{3/2}]}{Im[M_{1+}^{3/2}]} \quad (3)$$

$$R_{SM} = \frac{Im[S_{1+}^{3/2}]}{Im[M_{1+}^{3/2}]} \quad (4)$$

Here the standard notations ($A_{\ell\pm}^T$ with $A = M, E, S$)[6] of the multipole amplitudes are used in the right hand sides of the above equations. The R_{EM} and R_{SM} generated from the considered three models are compared in Fig.1 along with the empirical values obtained from performing the amplitude analyses of the data from MIT-Bates[7], Mainz[8], and Jefferson Laboratory (Jlab)[9, 10]. The comparison shown in Fig.1 was already given in the publication[10] by the Jlab CLAS collaboration.

We see from Fig.1 that the R_{SM} (right panel) ratios predicted by the SL model (solid curve) and DMT model (dashed curve) are strikingly different in the $Q^2 \leq 0.5$ (GeV/c)²

region. However their corresponding predictions of the ratio R_{EM} (left panel) are very close in the same low Q^2 region. As we will see in Figs.3-10, all three models give almost the same M_{1+} amplitude at the resonance position $W = 1232$ MeV. Thus their differences seen in Fig.1 can be understood from Fig.2 where the Q^2 -dependence of the predicted ratios $Im[S_{1+}]/Im[E_{1+}]$ are compared. We see that the SL model prediction at $Q^2 = 0$ is very close to the long wavelength limit $S_{1+} \sim E_{1+}$ ($L_{1+} = (\omega/|\vec{q}|)S_{1+}$) which is consistent with the results given in the papers by Amaldi, Fubini, and Furlan[11] and also by Capstick and Karl[12]. On the other hand, the $Im[S_{1+}]/Im[E_{1+}]$ of DMT(MAID2003) model approaches to 2 (3) at $Q^2 = 0$. Thus their predictions of R_{SM} are very different, as seen in the right panel of Fig.1.

As explained in section IV of Ref.[2], the long wave length limit is used in the SL model to define the bare $C2$ transition strength as $G_C(0) = -[4m_\Delta^2/(m_\Delta^2 - m_N^2)]G_E(0)$. With $G_E(0) = +0.025$ determined from fitting the pion photoproduction data, $G_C(0) = -0.238$ is fixed in the SL model *without* making use of the pion electroproduction data. In Fig.1 we see that the R_{SM} data point at $Q^2 \sim 0.127$ (GeV/c)² from MIT-Bates[7] and Mainz[8] disagrees with the prediction from the SL model, while it agrees with the results generated from the DMT and MAID models. This difference between the SL model and the DMT model marks the large discrepancies between these two dynamical models in describing the pion cloud effects. As illustrated in Fig.10 of Ref.[2], the pion cloud effect can enhance the $\gamma N \rightarrow \Delta$ $C2$ transition ($\sim Im(S_{1+}^{3/2})$) by a factor of about 2 at $Q^2 \sim 0.2$ (GeV/c)² and has a very pronounced Q^2 -dependence. Thus the experimental verifications of the predictions in the entire low Q^2 region given in Fig.1 will lead to a detailed understanding of the pion cloud effects.

II. MULTIPOLE AMPLITUDES

To give more detailed information for analyzing the new data, we compare in Figs. 3-10 the multipole amplitudes generated from the SL model (solid curves), DMT model (dashed curves), and MAID2003(dotted curves). We see that they are in excellent agreement only in the imaginary part of the M1 multipole (ImM_{1+}). For other resonant multipole amplitudes (E_{1+} and S_{1+}), the SL model differs significantly from the other two models. These differences can lead to rather different predictions on various interference cross sections σ_{LT} ,

σ_{TT} , and σ'_{LT} .

For non-resonant multipole amplitudes in Figs.3-10, the differences between the considered three models are very large in some cases. However it is not easy to identify experimental observables which are most effective in testing these weaker amplitudes.

Finally, we list in Tables 1-4 the multipoles amplitudes generated from the SL model at $Q^2 = 0., 0.05, 0.1, 0.20, 0.5$. The corresponding values from DMT and MAID can be obtained from the web site listed in Ref.[5]. More results from the SL model can be obtained from the authors.

This work was supported in part by the U.S. Department of Energy, Office of Nuclear Physics, under Contract No. W-31-109-ENG-38 and Japan Society for the Promotion of Science, Grant-in-Aid for Scientific Research (C) 15540275.

-
- [1] T. Sato and T.-S. H. Lee, Phys. Rev. C **54**, 2660 (1996).
- [2] T. Sato and T.-S. H. Lee, Phys. Rev. C **63**, 055201 (2001).
- [3] S. Kamalov and S. N. Yang, Phys. Rev. Lett **83**, 4494 (1999)
- [4] S. Kamalov et. al., Phys. Rev. **C64**, 032201 (2001)
- [5] D. Dreschel et al., Nucl. Phys. **A645**, 145 (1999);
<http://www.kph.uni-mainz.de/T/maid/maid.html>; Here we show their results of 2003.
- [6] Particle Data Group, D. E. Groom et al., Eur. Phys. J. **C15**, 1 (2000).
- [7] C. Mertz et al., Phys. Rev. Lett **86**, 2963 (2001).
- [8] R. Beck et al., Phys. Rev. **C61**, 035204 (2000); T. Pospischil et al., Phys. Rev. Lett. **86**, 2959 (2001).
- [9] V.V. Frolov et al., Phys. Rev. Lett. **82**, 45 (1999)
- [10] K. Joo et. al., Phys. Rev. Lett. **88**, 12201 (2002)
- [11] See Eq.(C13) of E. Amaldi, S. Fubini, and G. Furlan, in Springer Tracts in Mordern Physics, Vol. 83, edited by G. Hohler (Springer, Berline, 1979), p.1.
- [12] See second paragraph of Sec. III of S. Capstick and G. Karl, Phys. Rev. **D 41**, 2767 (1990).

TABLE I: The Q^2 -dependence of the multipole amplitude for the $\gamma + p \rightarrow \pi^0 + p$ reaction in unit of $10^{-3}/m_\pi$ at $W = 1.232\text{GeV}$. Q^2 is given in unit of $(\text{GeV}/c)^2$.

Q^2	0	0.05	0.1	0.2	0.5
E_0^+	$-0.346 + 2.105i$	$0.520 + 1.961i$	$1.169 + 1.786i$	$1.987 + 1.454i$	$2.630 + 0.837i$
E_1^+	$1.056 - 0.652i$	$1.067 - 0.808i$	$1.003 - 0.870i$	$0.848 - 0.846i$	$0.539 - 0.571i$
M_1^+	$-2.048 + 25.008i$	$-1.857 + 27.276i$	$-1.648 + 27.872i$	$-1.321 + 26.989i$	$-0.826 + 21.053i$
M_1^-	$-2.081 + 0.311i$	$-2.508 + 0.242i$	$-2.792 + 0.183i$	$-3.097 + 0.103i$	$-3.118 + 0.011i$
S_0^+	$-1.461 + 1.784i$	$-1.351 + 1.784i$	$-1.281 + 1.641i$	$-1.230 + 1.332i$	$-1.131 + 0.779i$
S_1^+	$0.819 - 0.557i$	$0.832 - 0.922i$	$0.735 - 1.122i$	$0.540 - 1.257i$	$0.262 - 1.174i$
S_1^-	$0.985 + 0.407i$	$1.430 + 0.460i$	$1.724 + 0.449i$	$2.014 + 0.385i$	$1.988 + 0.233i$

TABLE II: The Q^2 -dependence of the multipole amplitude for the $\gamma + p \rightarrow \pi^+ + n$ reaction.

Q^2	0	0.05	0.1	0.2	0.5
E_0^+	$-10.665 - 0.450i$	$-10.320 - 0.601i$	$-9.718 - 0.699i$	$-8.384 - 0.793i$	$-5.509 - 0.779i$
E_1^+	$-1.448 - 0.441i$	$-1.452 - 0.552i$	$-1.358 - 0.596i$	$-1.140 - 0.583i$	$-0.723 - 0.394i$
M_1^+	$1.144 + 17.660i$	$0.715 + 19.269i$	$0.376 + 19.695i$	$-0.024 + 19.076i$	$-0.308 + 14.884i$
M_1^-	$-3.601 + 0.135i$	$-2.148 + 0.156i$	$-0.946 + 0.170i$	$0.610 + 0.185i$	$2.161 + 0.182i$
S_0^+	$-8.502 - 0.128i$	$-8.555 - 0.152i$	$-7.852 - 0.132i$	$-6.283 - 0.065i$	$-3.485 + 0.051i$
S_1^+	$-1.120 - 0.378i$	$-1.113 - 0.636i$	$-0.962 - 0.780i$	$-0.676 - 0.879i$	$-0.288 - 0.826i$
S_1^-	$-7.513 - 0.040i$	$-8.714 - 0.063i$	$-8.754 - 0.081i$	$-7.908 - 0.100i$	$-5.370 - 0.106i$

TABLE III: The Q^2 -dependence of the multipole amplitude for the $\gamma + n \rightarrow \pi^0 + n$ reaction.

Q^2	0	0.05	0.1	0.2	0.5
E_0^+	$2.188 + 2.576i$	$2.478 + 2.325i$	$2.666 + 2.065i$	$2.811 + 1.607i$	$2.518 + 0.816i$
E_1^+	$1.052 - 0.652i$	$1.050 - 0.808i$	$0.974 - 0.869i$	$0.799 - 0.846i$	$0.471 - 0.570i$
M_1^+	$-3.374 + 25.020i$	$-3.286 + 27.289i$	$-3.092 + 27.886i$	$-2.690 + 27.001i$	$-1.820 + 21.062i$
M_1^-	$-0.905 + 0.357i$	$-1.193 + 0.295i$	$-1.410 + 0.238i$	$-1.685 + 0.160i$	$-1.853 + 0.061i$
S_0^+	$0.995 + 2.241i$	$1.425 + 2.301i$	$1.649 + 2.186i$	$1.760 + 1.888i$	$1.458 + 1.260i$
S_1^+	$0.834 - 0.557i$	$0.850 - 0.922i$	$0.755 - 1.123i$	$0.559 - 1.257i$	$0.267 - 1.174i$
S_1^-	$0.268 + 0.379i$	$0.441 + 0.420i$	$0.536 + 0.401i$	$0.582 + 0.328i$	$0.416 + 0.170i$

 TABLE IV: The Q^2 -dependence of the multipole amplitude for the $\gamma + n \rightarrow \pi^- + p$ reaction.

Q^2	0	0.05	0.1	0.2	0.5
E_0^+	$-14.247 - 1.116i$	$-13.089 - 1.117i$	$-11.835 - 1.092i$	$-9.549 - 1.010i$	$-5.350 - 0.749i$
E_1^+	$-1.443 - 0.441i$	$-1.428 - 0.552i$	$-1.317 - 0.596i$	$-1.071 - 0.583i$	$-0.627 - 0.394i$
M_1^+	$3.018 + 17.642i$	$2.735 + 19.250i$	$2.419 + 19.676i$	$1.912 + 19.058i$	$1.098 + 14.871i$
M_1^-	$-5.265 + 0.068i$	$-4.009 + 0.082i$	$-2.900 + 0.092i$	$-1.388 + 0.105i$	$0.372 + 0.110i$
S_0^+	$-11.975 - 0.774i$	$-12.481 - 0.882i$	$-11.995 - 0.902i$	$-10.512 - 0.852i$	$-7.146 - 0.630i$
S_1^+	$-1.141 - 0.378i$	$-1.139 - 0.636i$	$-0.989 - 0.780i$	$-0.702 - 0.879i$	$-0.296 - 0.826i$
S_1^-	$-6.500 + 0.001i$	$-7.316 - 0.007i$	$-7.074 - 0.014i$	$-5.882 - 0.020i$	$-3.146 - 0.017i$

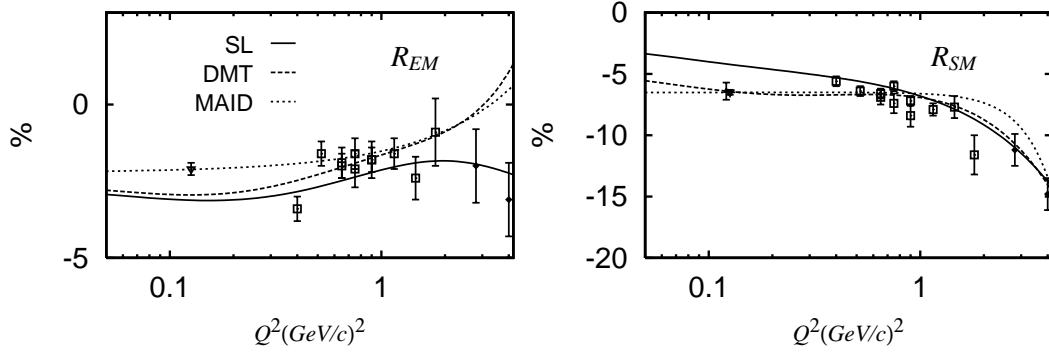


FIG. 1: The ratios R_{EM} (left panel) and R_{SM} (right panel) predicted by the SL model[1,2] (solid curves), DMT model[3,4] (dashed curves), and MAID2003[5] (dotted curves) are compared with the empirical values from MIT-Bates[7], Mainz[8], and Jefferson Laboratory[9,10].

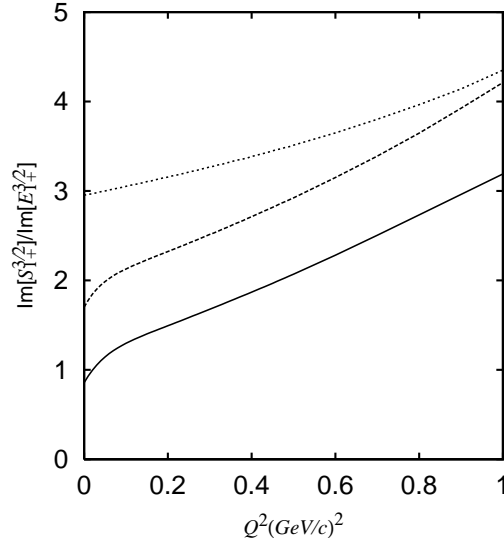


FIG. 2: The ratios $\text{Im}(S_{1+}^{3/2})/\text{Im}(E_{1+}^{3/2})$ predicted by the SL model[1,2] (solid curves), DMT model[3,4] (dashed curves), and MAID2003[5] (dotted curves) are compared.

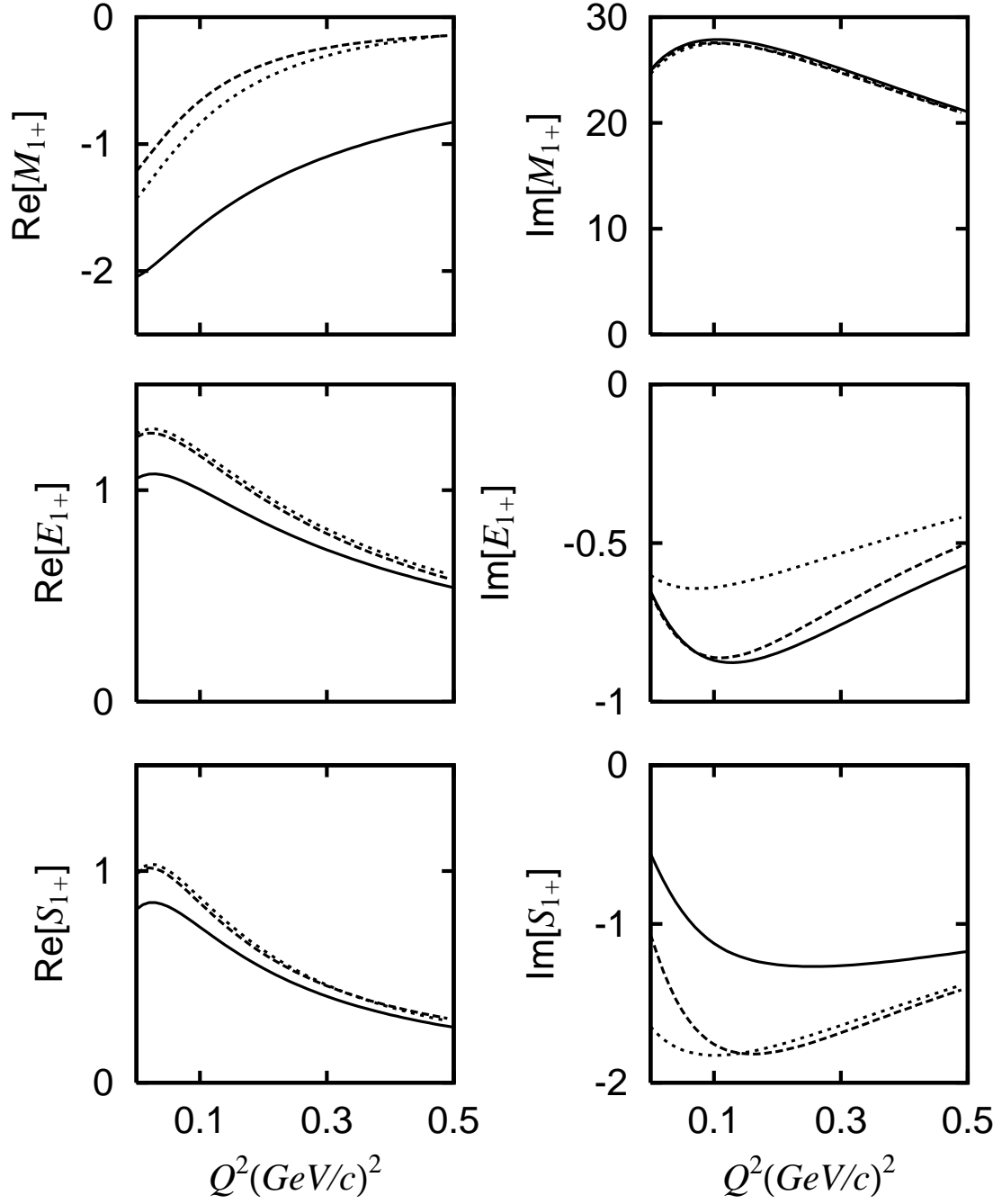


FIG. 3: Resonant multipole amplitudes of the $\gamma + p \rightarrow \pi^0 + p$ reaction at $W = 1232$ MeV.

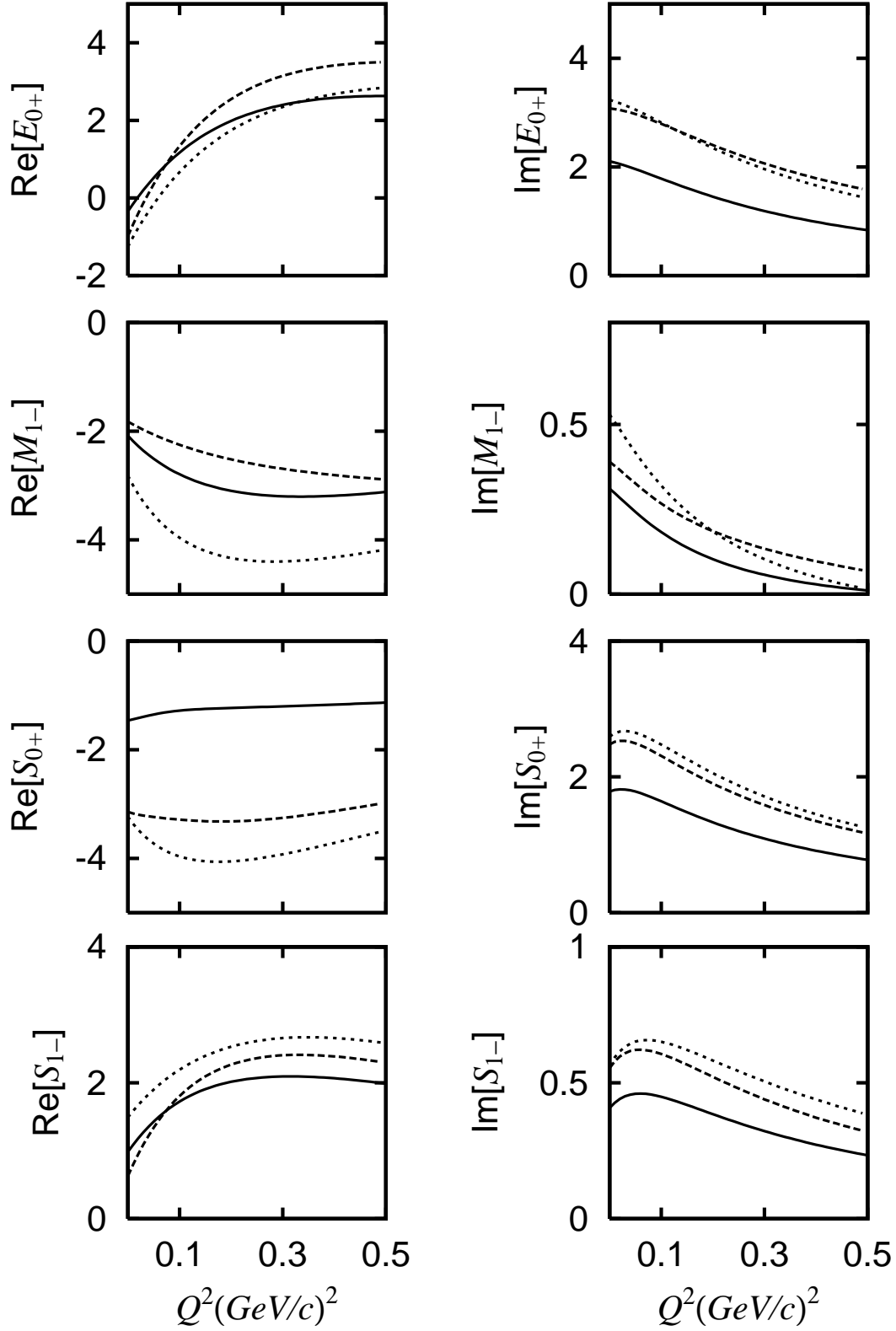


FIG. 4: Non-resonant multipole amplitudes of the $\gamma^* p \rightarrow \pi^0 p$ reaction at $W = 1232$ MeV.

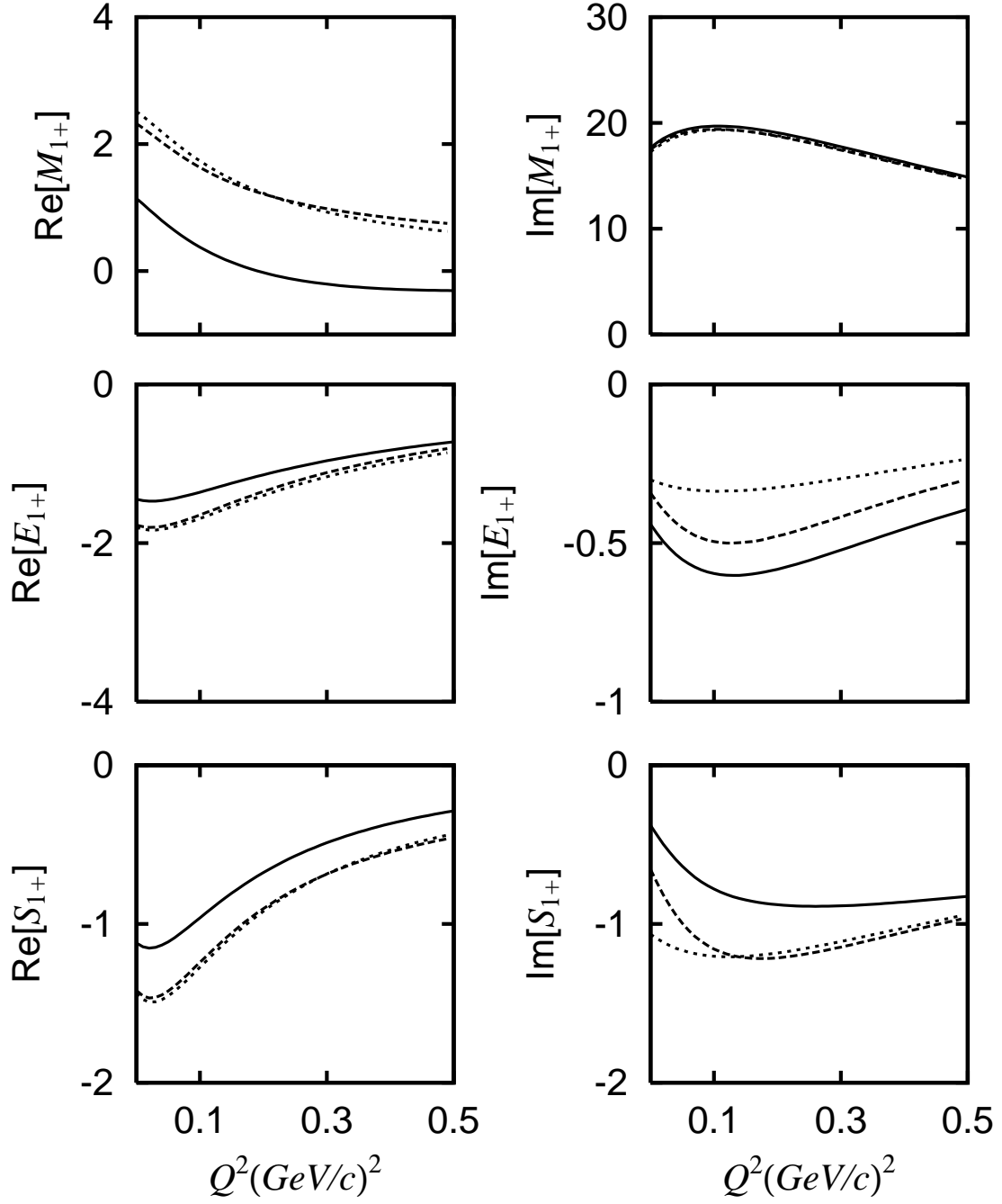


FIG. 5: Resonant multipole amplitudes of the $\gamma^* p \rightarrow \pi^+ n$ reaction at $W = 1232$ MeV.

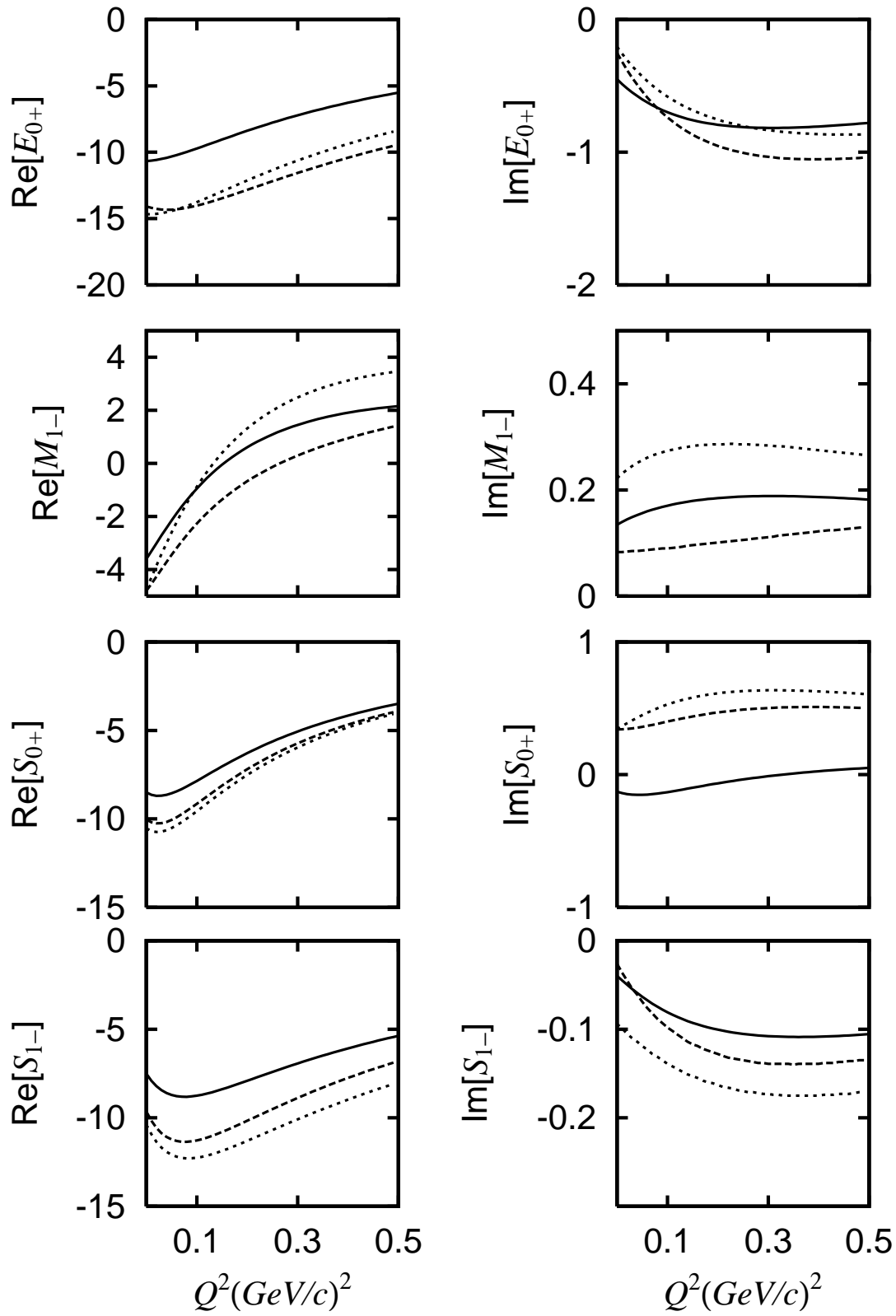


FIG. 6: Non-resonant multipole amplitudes of the $\gamma^*p \rightarrow \pi^+n$ reaction at $W = 1232$ MeV.

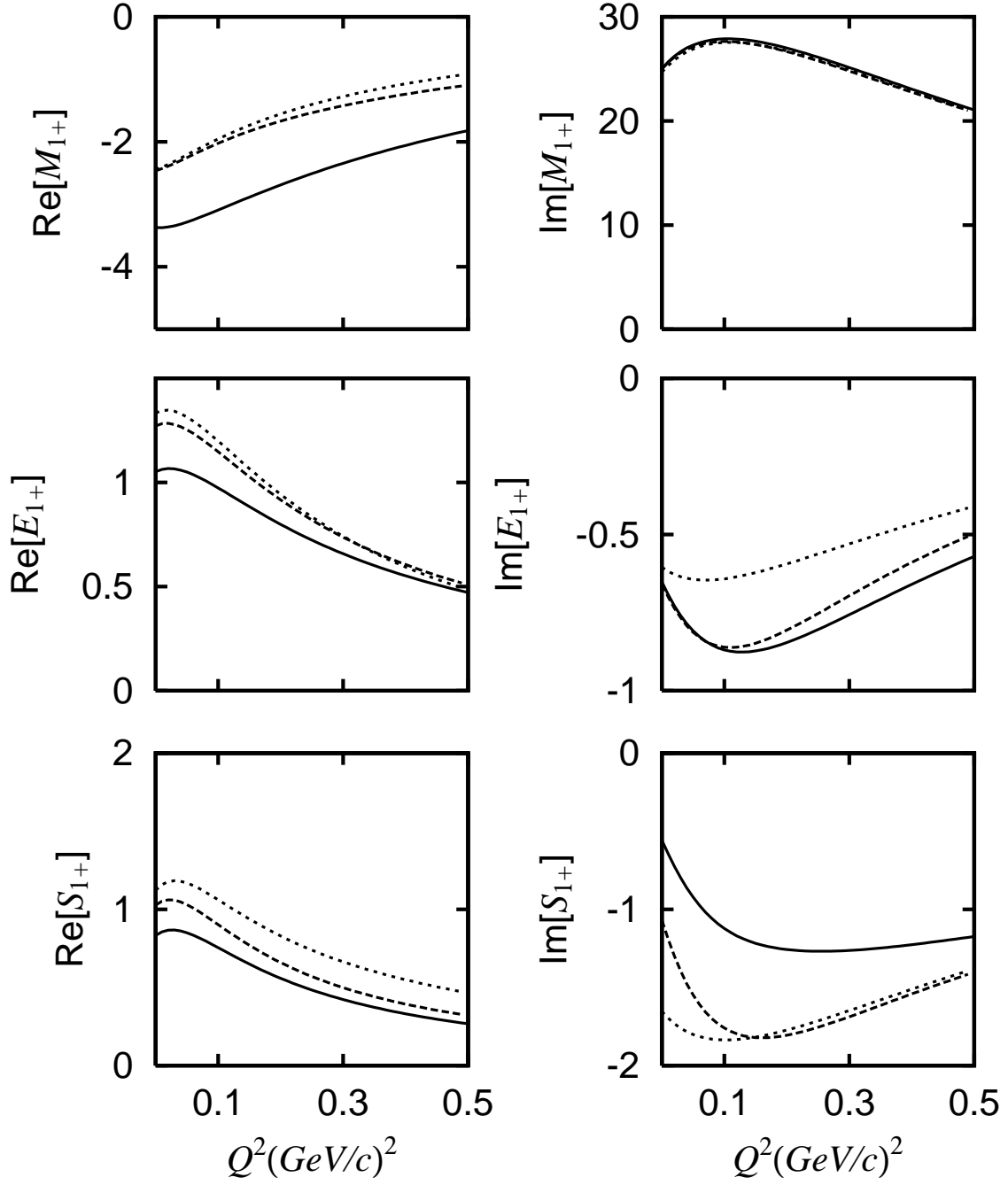


FIG. 7: Resonant multipole amplitudes of the $\gamma^* n \rightarrow \pi^0 n$ reaction at $W = 1232$ MeV.

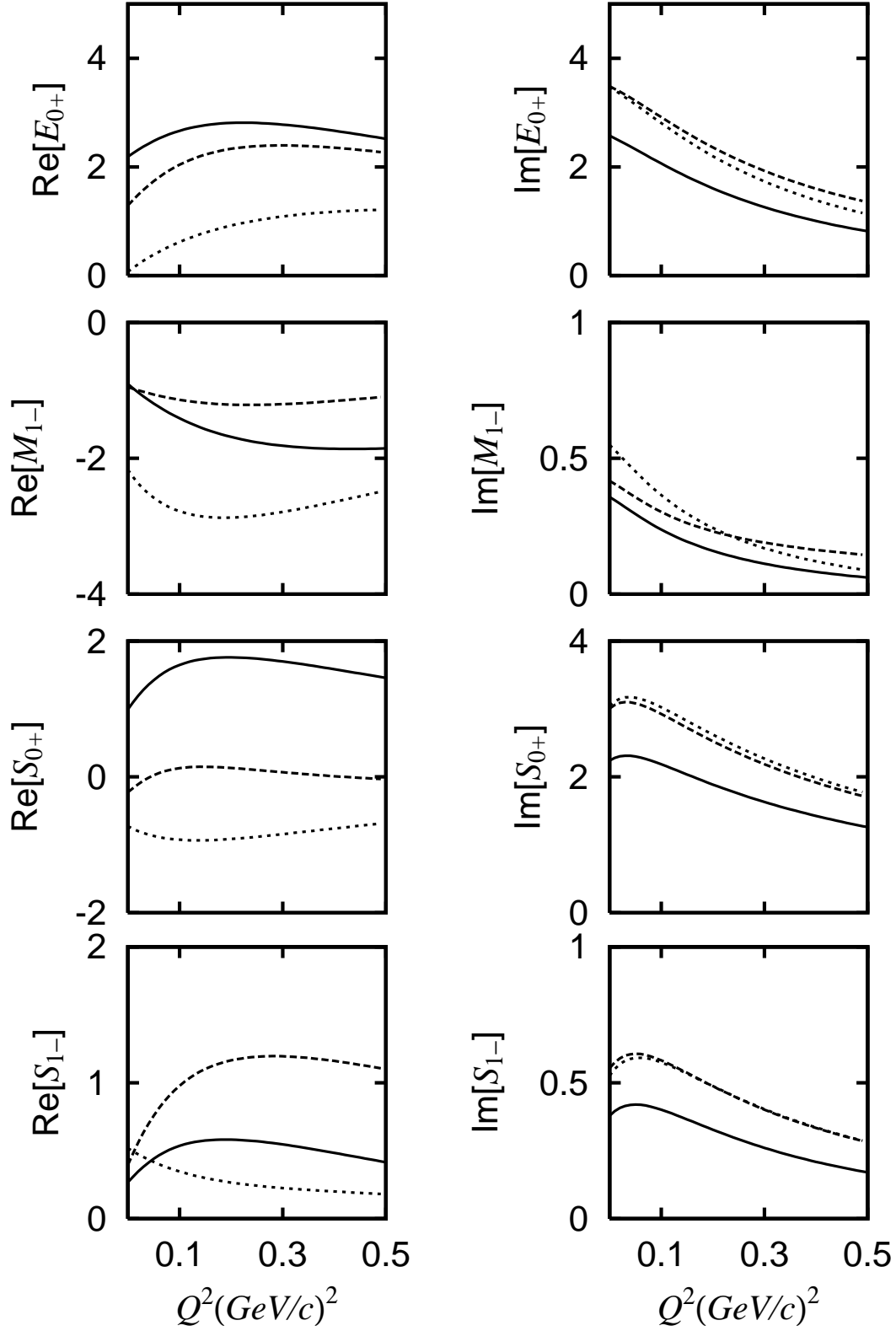


FIG. 8: Non-resonant multipole amplitudes of the $\gamma^* n \rightarrow \pi^0 n$ reaction at $W = 1232$ MeV.

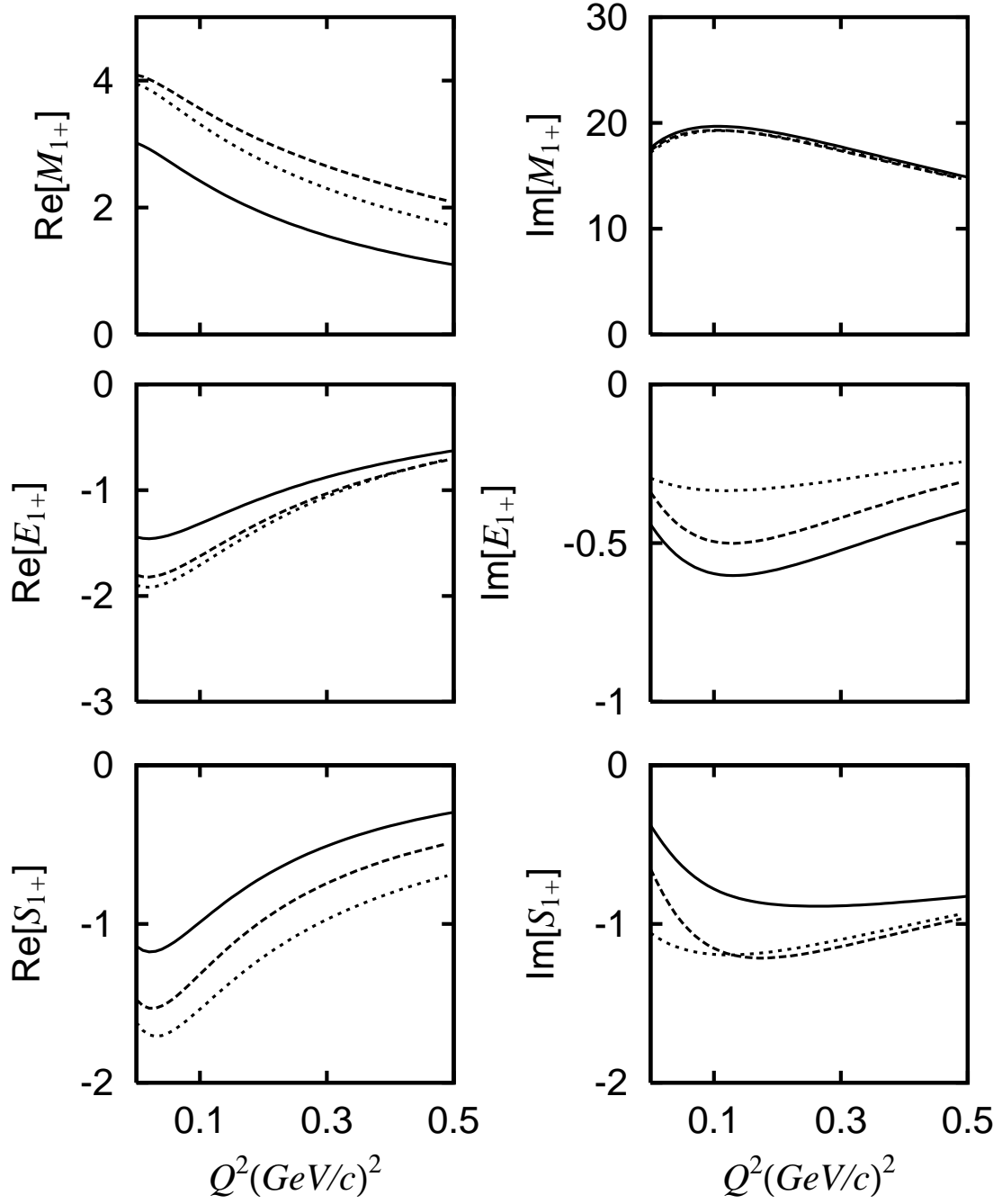


FIG. 9: Resonant multipole amplitudes of the $\gamma^* n \rightarrow \pi^- p$ reaction at $W = 1232$ MeV.

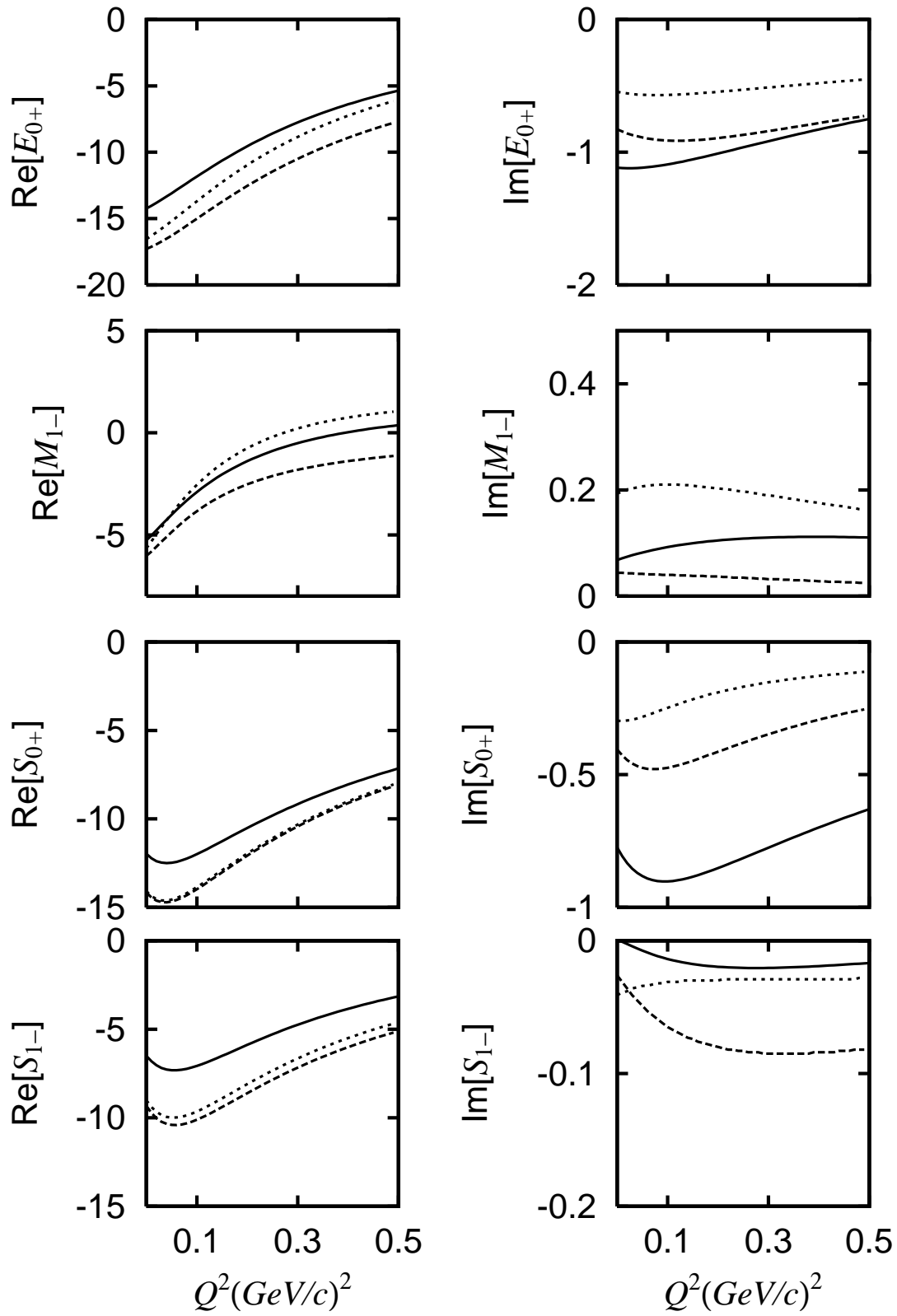


FIG. 10: Non-resonant multipole amplitudes of the $\gamma^* n \rightarrow \pi^- p$ reaction at $W = 1232$ MeV.